NuFact 2024

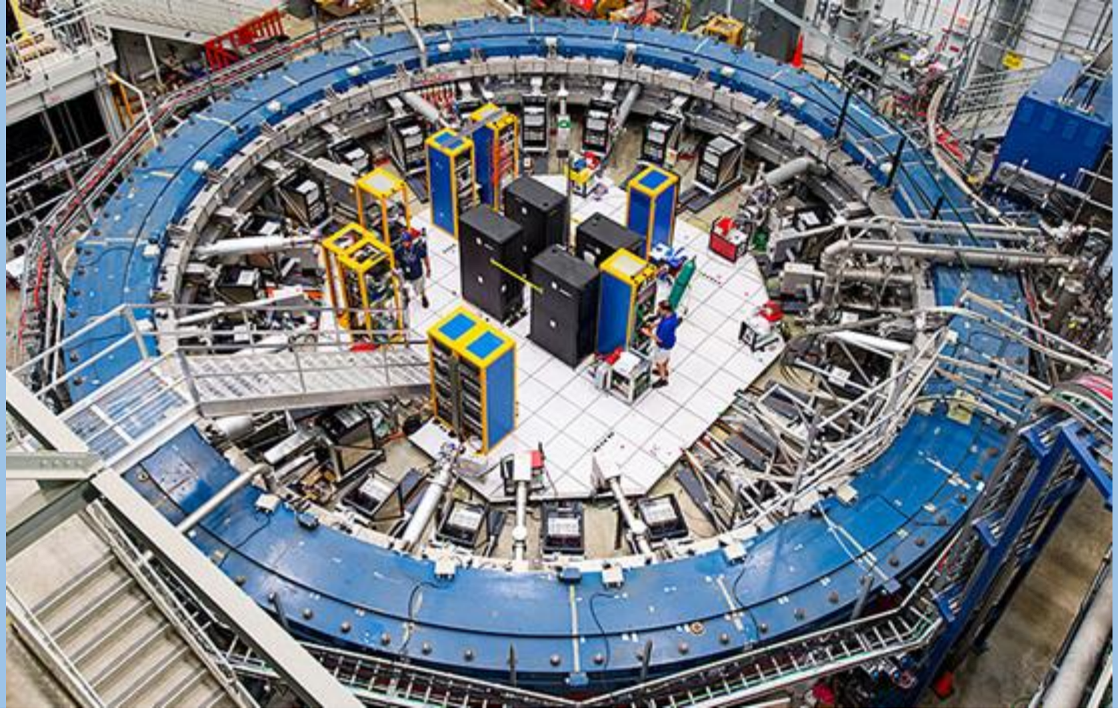

Beam Dynamics Corrections of the Muon *g-2* Experiment at Fermilab

David A. Tarazona

September 16, 2024

Recap

$$a_\mu = \frac{\omega_a}{\tilde{\omega}'_p(T_r)} \frac{\mu'_p(T_r)}{\mu_e(H)} \frac{\mu_e(H)}{\mu_e} \frac{m_\mu}{m_e} \frac{g_e}{2}$$

Quantities measured outside of the experiment, with **25 ppb precision**.

Unblinding conversion factor

On Kim

This talk

$$\mathcal{R}'_\mu = \frac{\omega_a}{\tilde{\omega}'_p(T_r)} = \frac{f_{\text{clock}}\, \omega_a^m (1 + C_e + C_p + C_{pa} + C_{dd} + C_{ml})}{f_{\text{calib}} \langle \omega_p(x,y,\phi) \times M(x,y,\phi) \rangle (1 + B_k + B_q)}$$

NMR probe calibration factor

David Kessler

Motivation/Outline

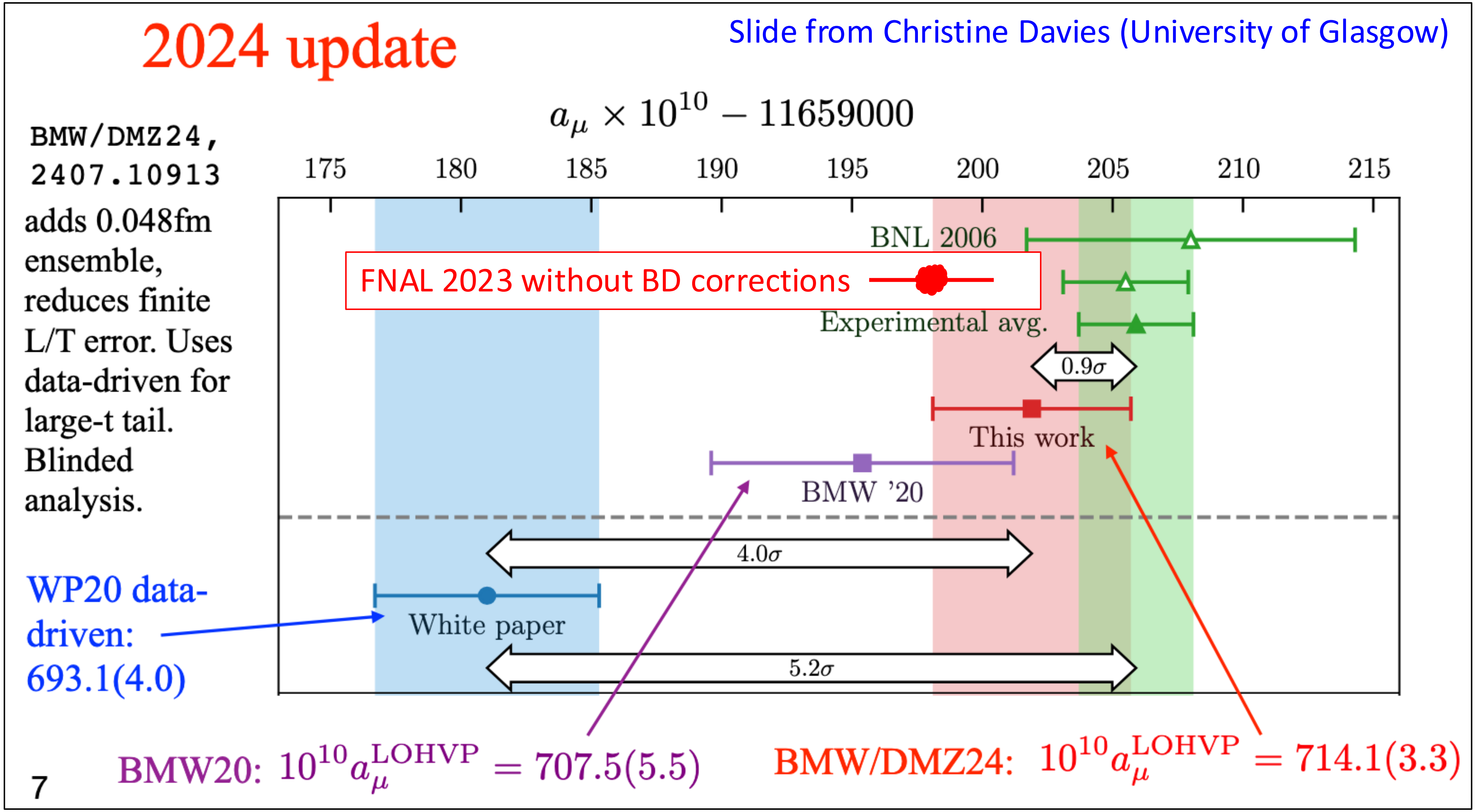

Motivation/Outline

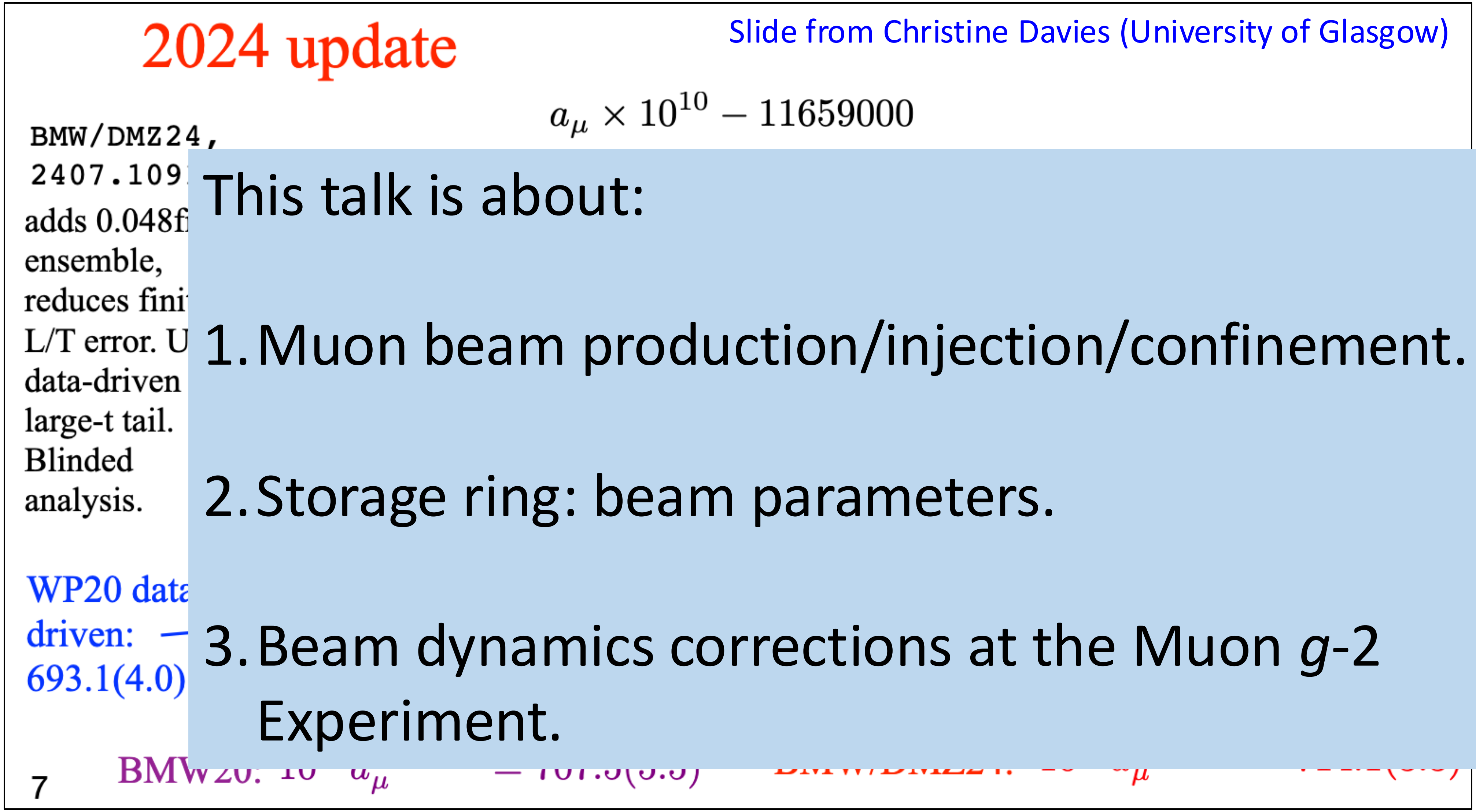

Slide from Christine Davies (University of Glasgow)

This talk is about:

1. Muon beam production/injection/confinement.
2. Storage ring: beam parameters.
3. Beam dynamics corrections at the Muon *g*-2 Experiment.

Muon beam production

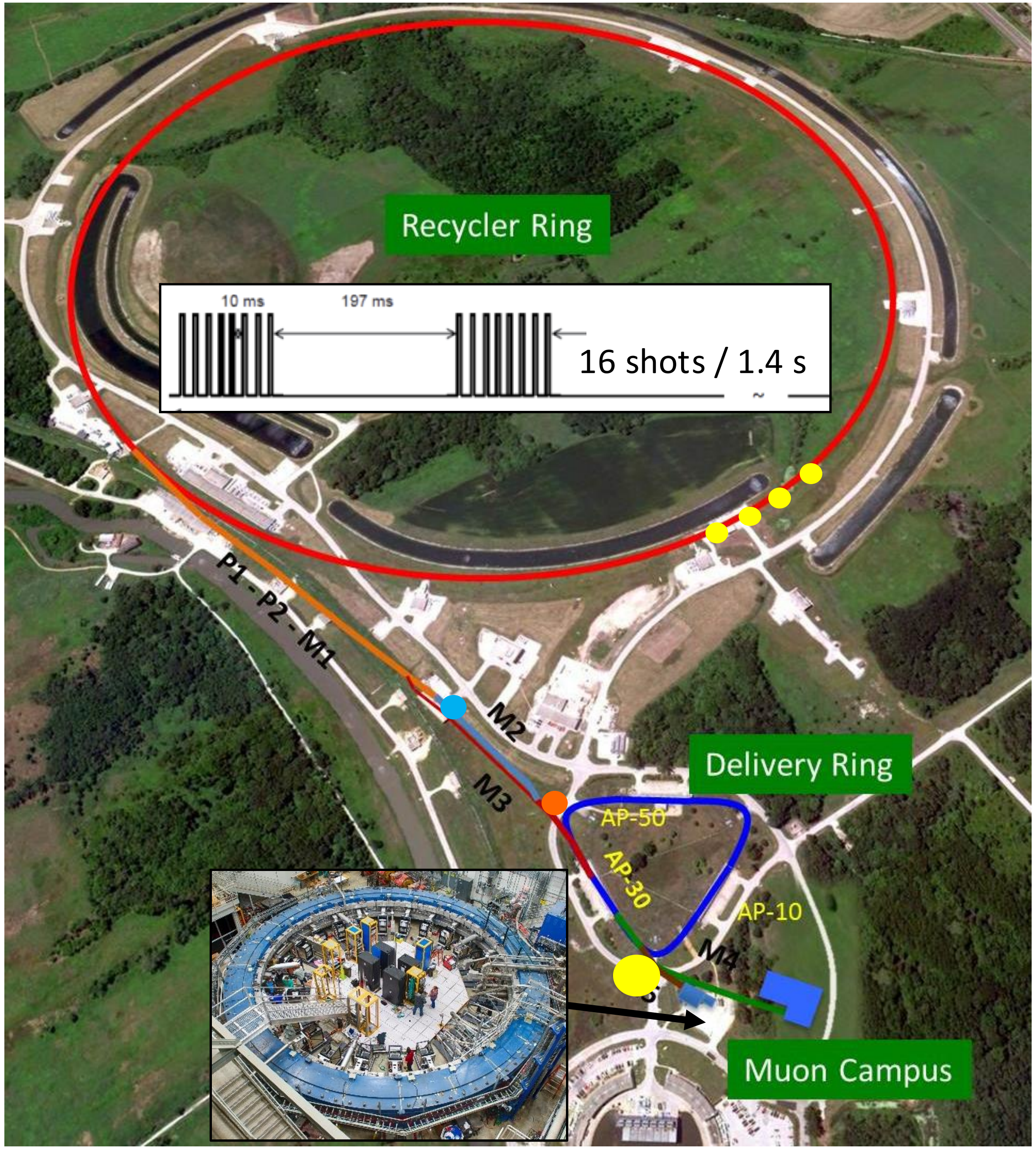

- 10^{12} protons per pulse (~8.89GeV) hit the production target.
- From parity violation in $\pi^+ \rightarrow \mu^+\nu_\mu$ decays, muons are highly polarized.
- Fermilab's Muon Campus beamlines transport ~3.1 GeV/c muons to storage ring.
- Muon beam is purified in Delivery Ring.

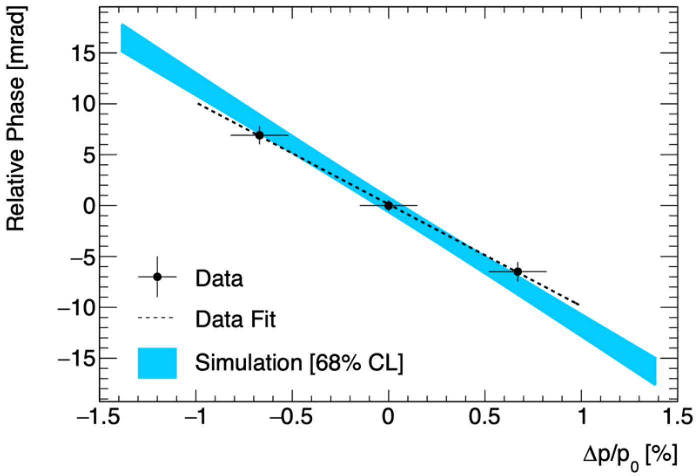

Muon Beam: Injection

- **Injection** kickers aim to align muons with storage region.

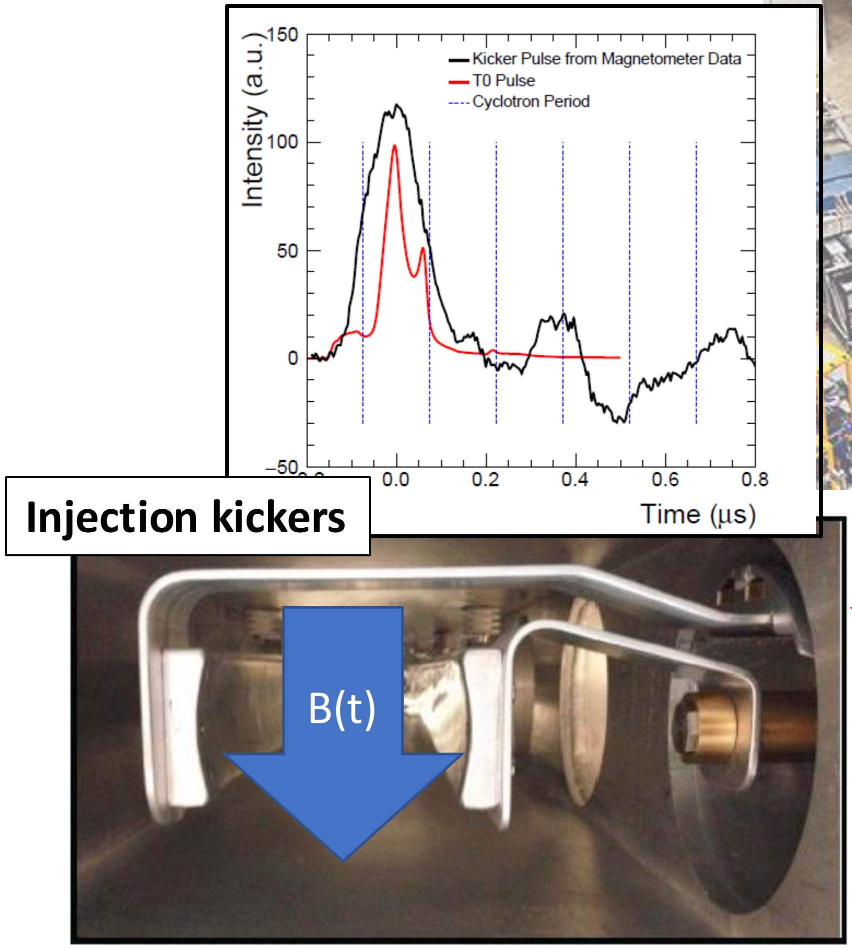

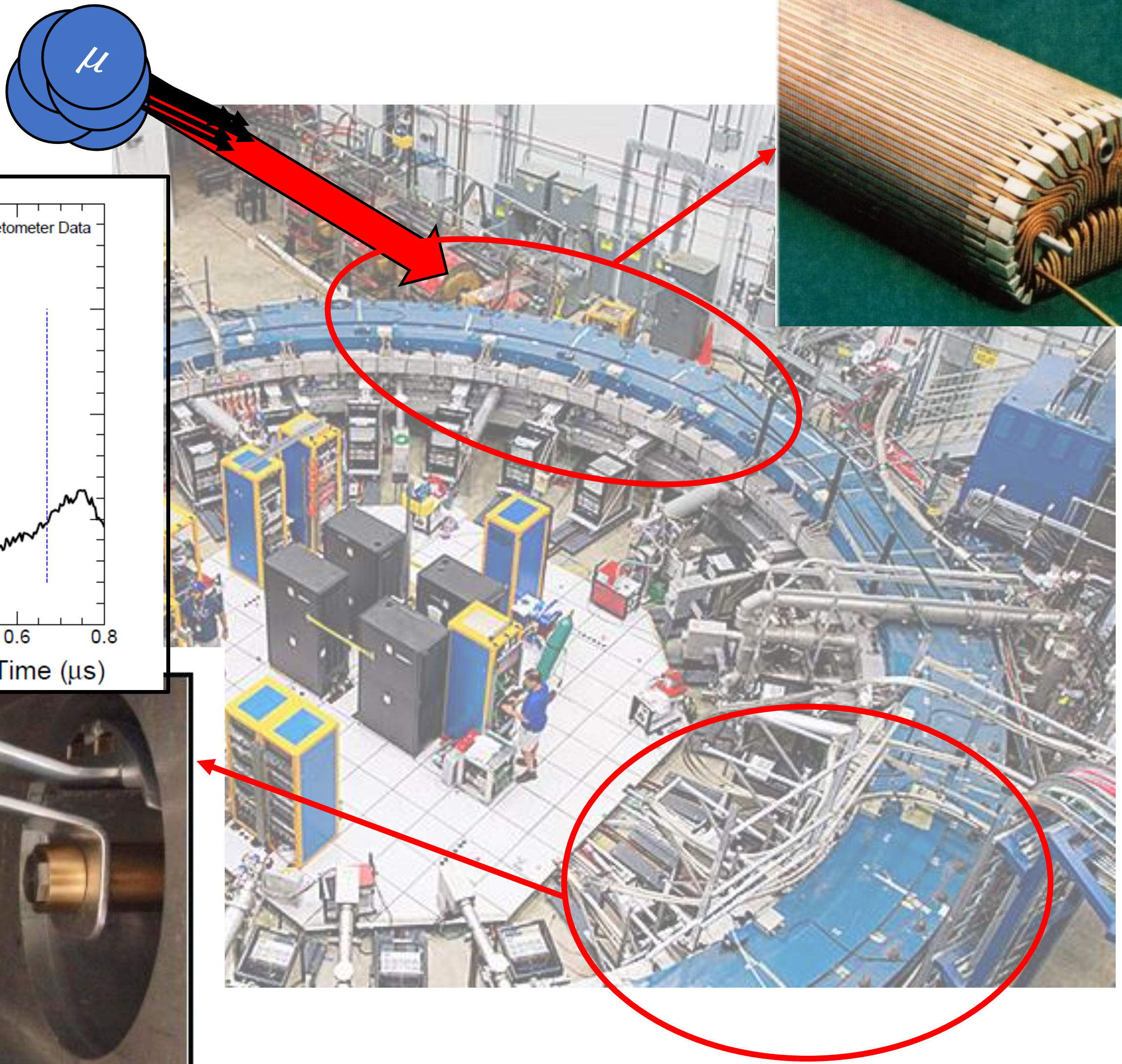

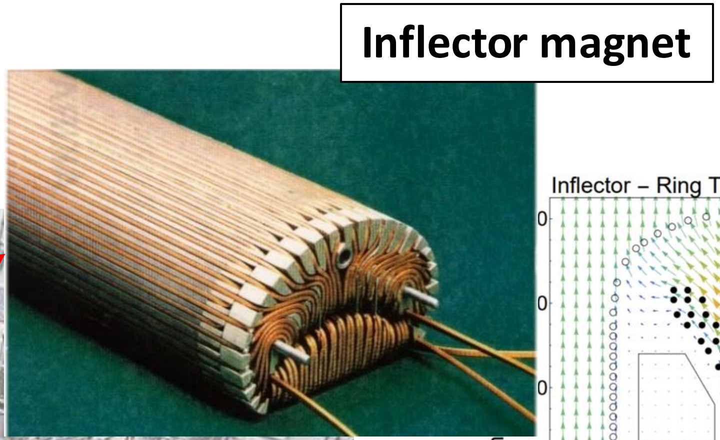

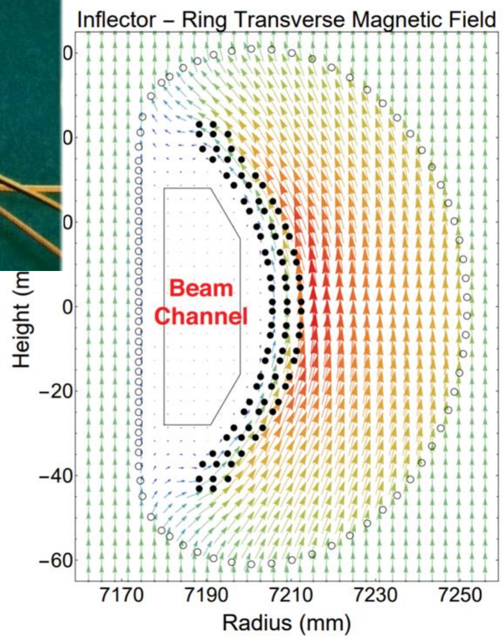

- **Inflector magnet** cancels the main focusing magnetic field (1.5 T) to inject the bunch directly.

Muon beam injection

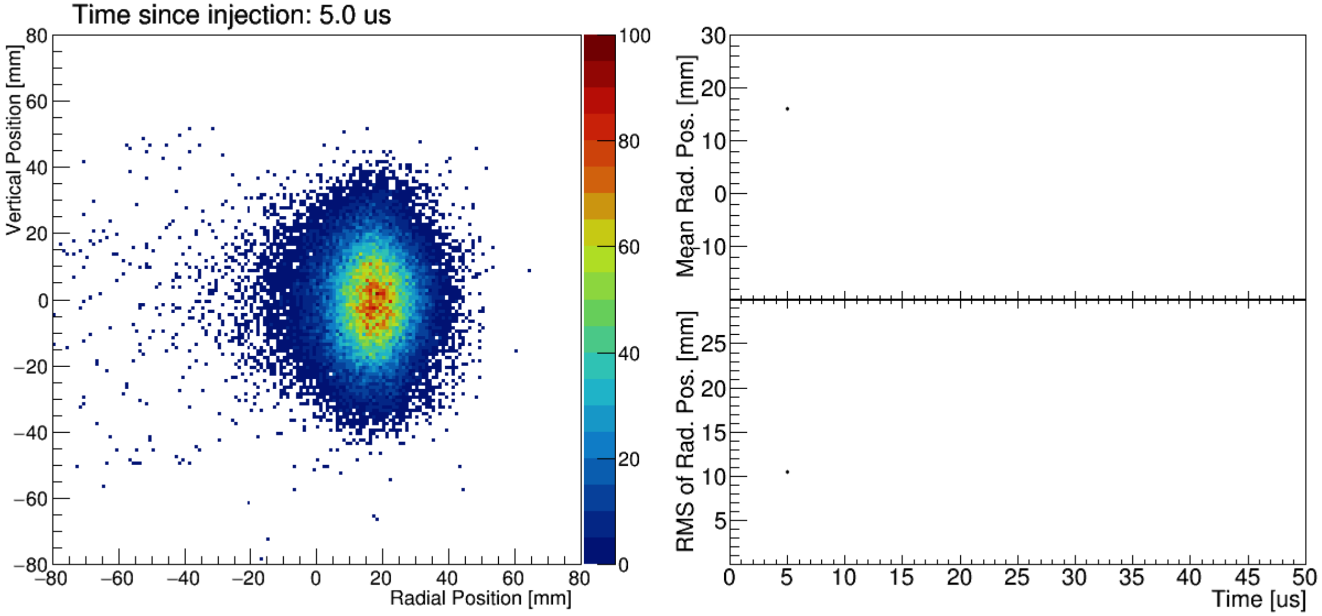

- Beam's transverse profile is measured with gaseous straw tracking detector:

Section through storage ring

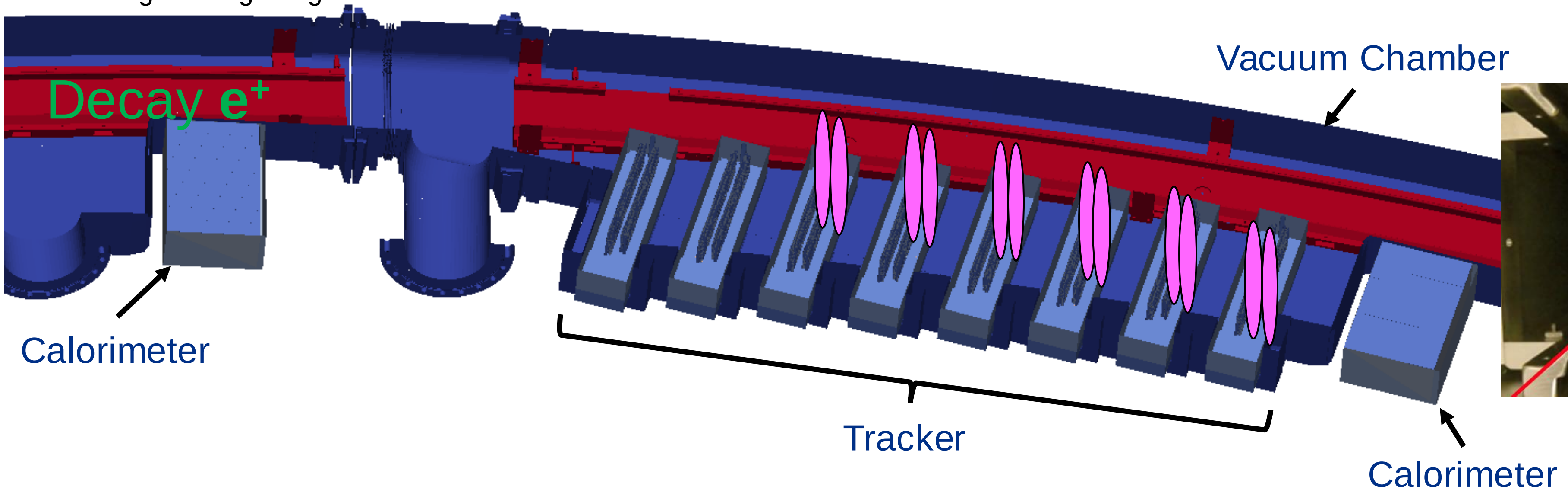

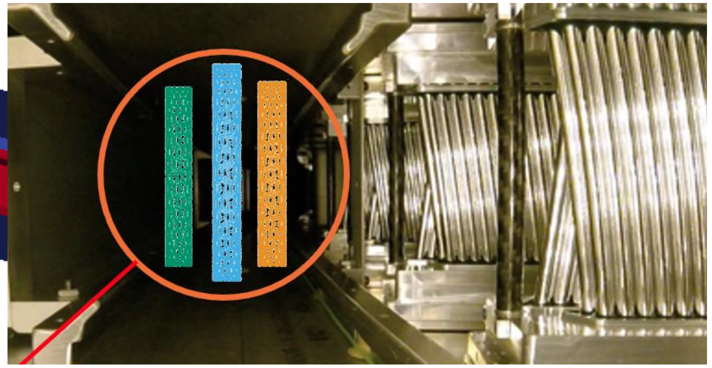

- Imperfect injection kick creates beam's radial centroid oscillation (aka "Coherent Betatron Oscillation" CBO).

$$f_{CBO} = f_C(1 - \nu_x) \approx 0.37 \text{ MHz}$$

- Optics mismatch between injected beam and ring produces beam's radial width oscillation.

- New application of radio-frequency (RF) electric fields minimizes CBO.

Muon beam vertical confinement

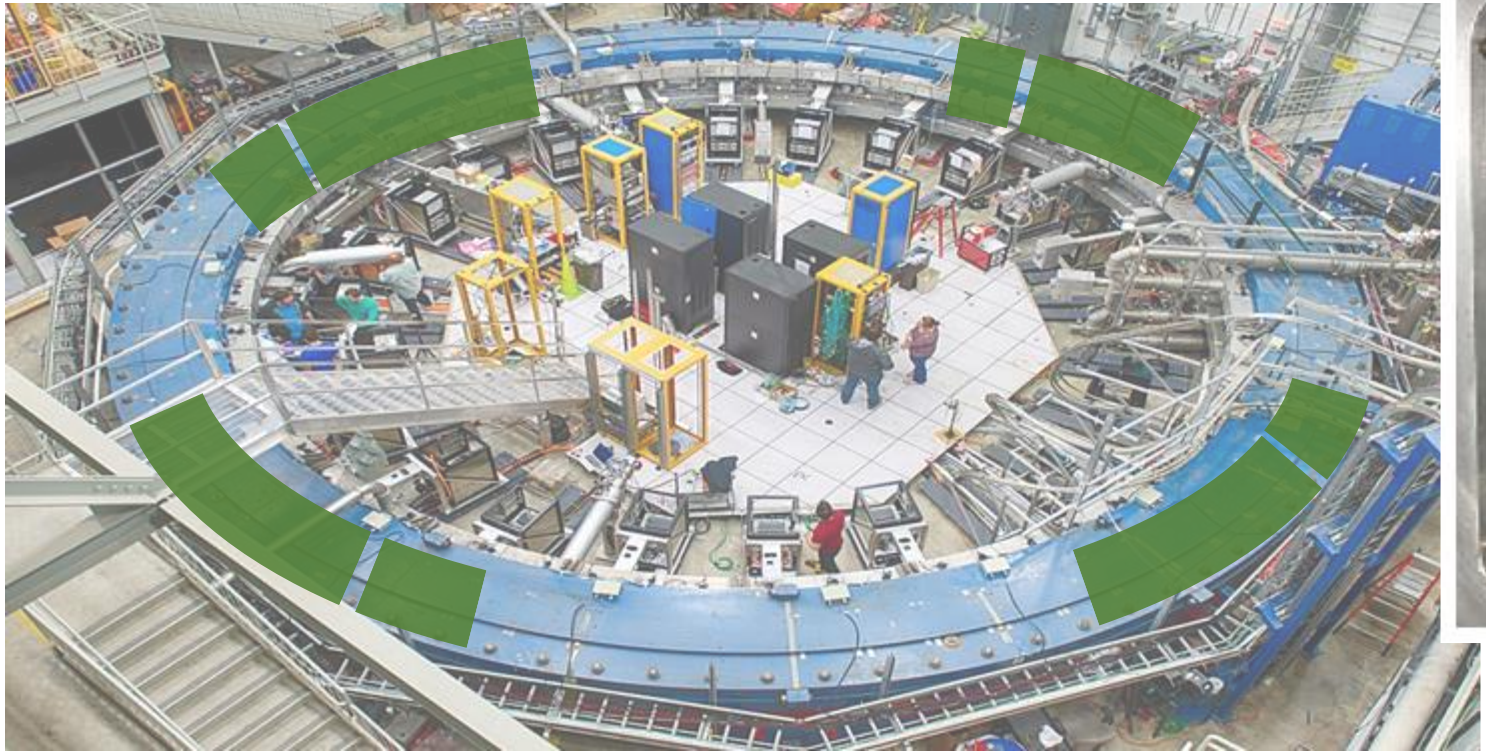

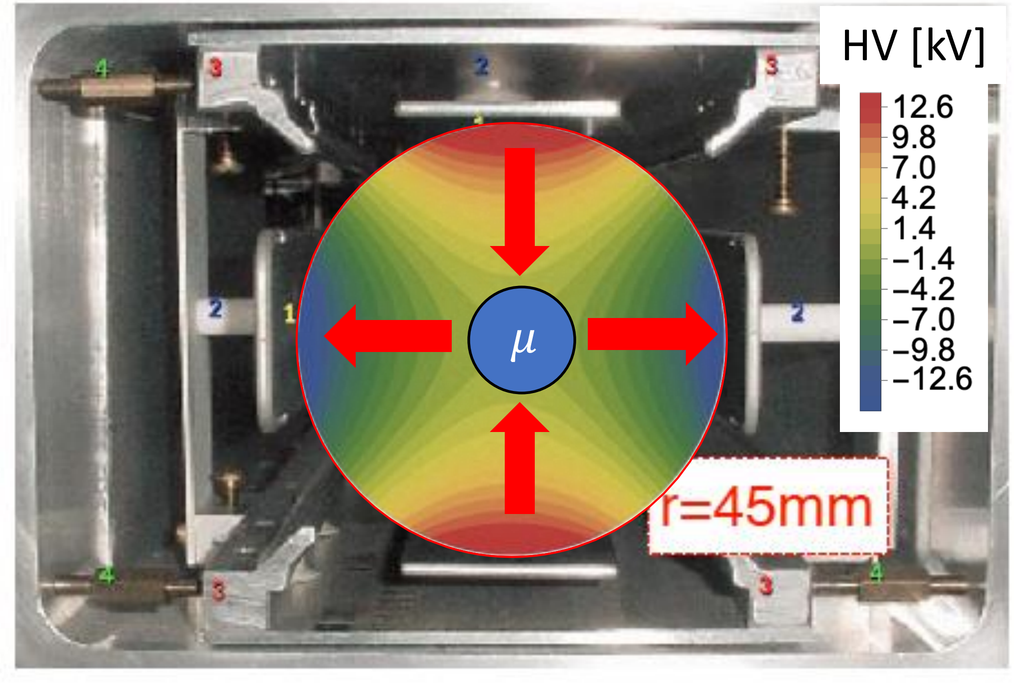

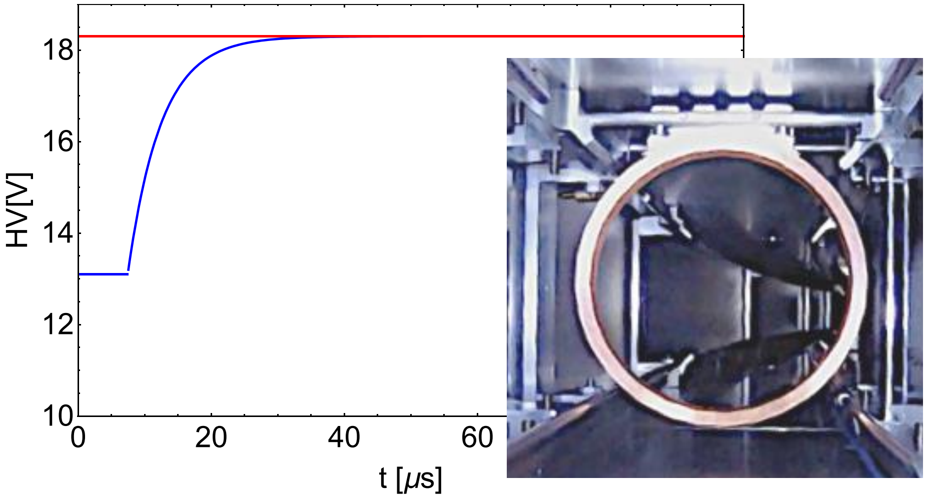

- The ElectroStatic Quadrupole system (ESQ) provides vertical focusing.
- The ESQ plates are mis-powered for closed orbit distortions.

Ring and optical lattice parameters

Parameter	Value
Nominal momentum (p_0)	3.094 GeV/c
Momentum acceptance	±0.56%
Radial tune (ν_x)	0.944
Vertical tune (ν_y)	0.330
Bending magnetic field (B_0)	1.4513 T
Bending radius (ρ_0)	7.112 m
Revolution period	149.2 ns
Horizontal admittance	268π mm.mrad
Vertical admittance	93π mm.mrad
Maximum excursion	45 mm
x' max	6 mrad
y' max	2 mrad
High-voltage (HV) setpoint	$\sim \pm 18.3$ kV
Vacuum in storage volume	$\lesssim 10^{-6}$ Torr
Current	5170 A

*Representative values

- Temporal stability and spatial homogeneity of the magnetic guide field are essential to the experiment.

- Average magnetic field experienced by stored muons needs to remain stable on the scale of ppm.

Parameter	Value (~)	Azimuthal Variation
α_x	0	$< \pm 0.1$
β_x	7.5 m	< 3%
γ_x	$0.13\,\mathrm{m}^{-1}$	< 3%
D_x	8 m	< 2%
α_y	0	$< \pm 0.2$
β_y	21.5 m	< 3%
γ_y	$0.046\,\mathrm{m}^{-1}$	< 1%
D_y	0.03 m	$< \pm 0.01$ m

*Representative values

Optical lattice

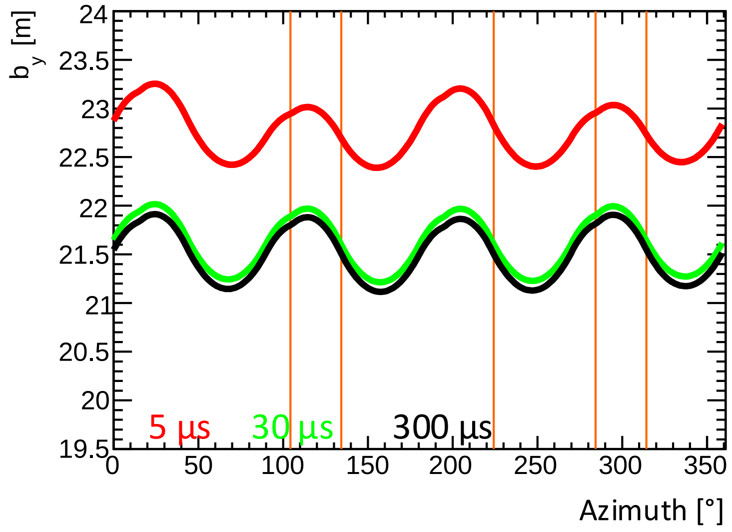

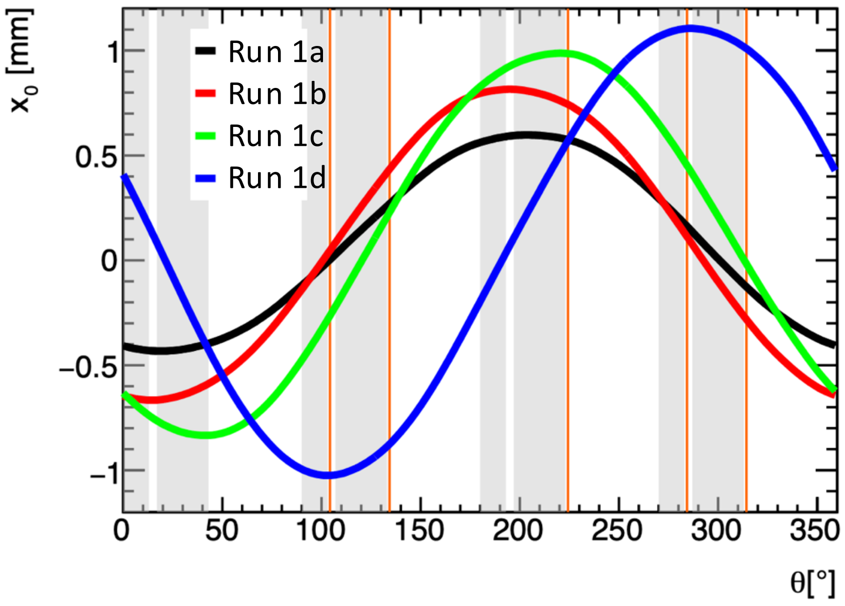

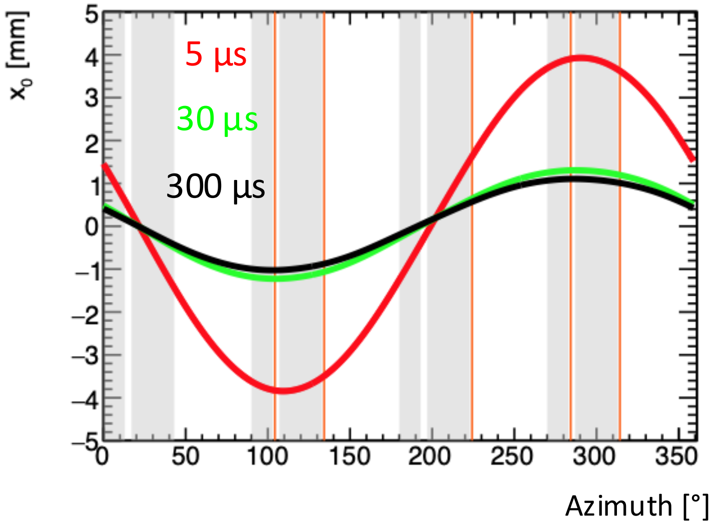

- Beam stability is provided by relatively weak focusing:

$$x'' + \frac{1-n}{\rho_0^2} x = 0$$
$$y'' + \frac{n}{\rho_0^2} y = 0$$

- Field index *n* from ESQ system:

$$n = \frac{\rho_0}{vB_0}\frac{\partial E_y}{\partial y}$$

$$n \approx 0.1 \quad , \quad 0 \leq n \leq 1$$

- Weak-focusing modelling provides 1st order ring representation:

$$\beta_x(s) \approx \frac{\rho_0}{\sqrt{1-n}} \qquad \beta_y(s) \approx \frac{\rho_0}{\sqrt{n}} \qquad D_x(s) \approx \frac{\rho_0}{1-n}$$

$$Q_y \approx \sqrt{n} \qquad Q_x \approx \sqrt{1-n}$$

Nonlinearities

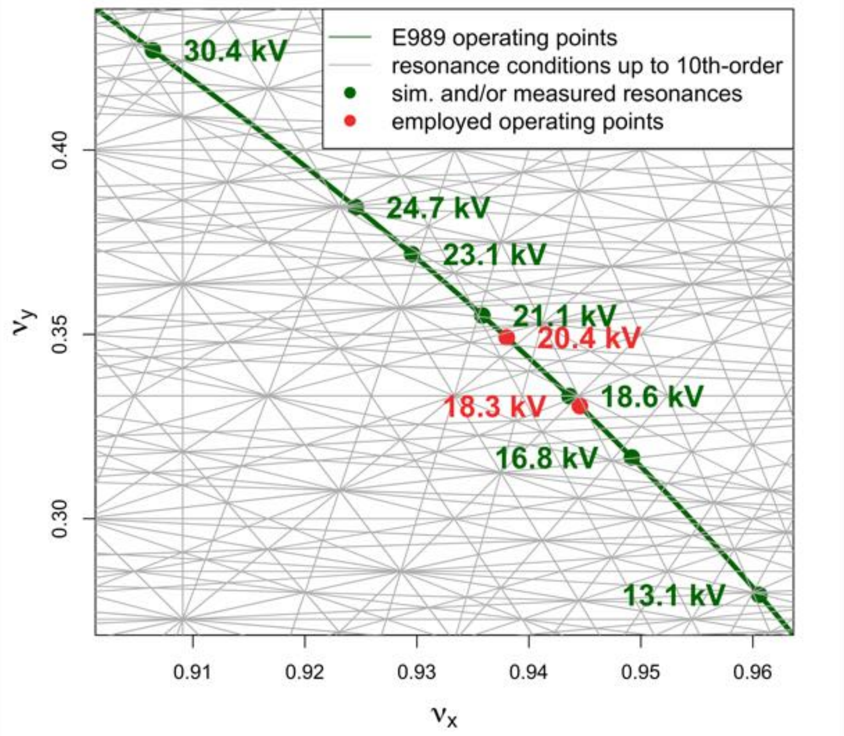

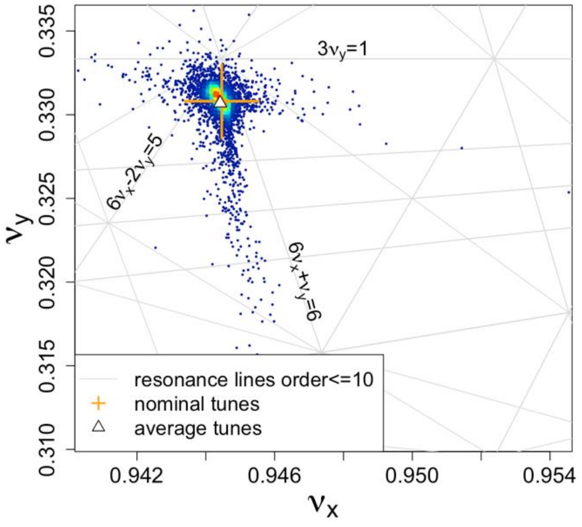

- Geometry of plates introduces nonlinearities.

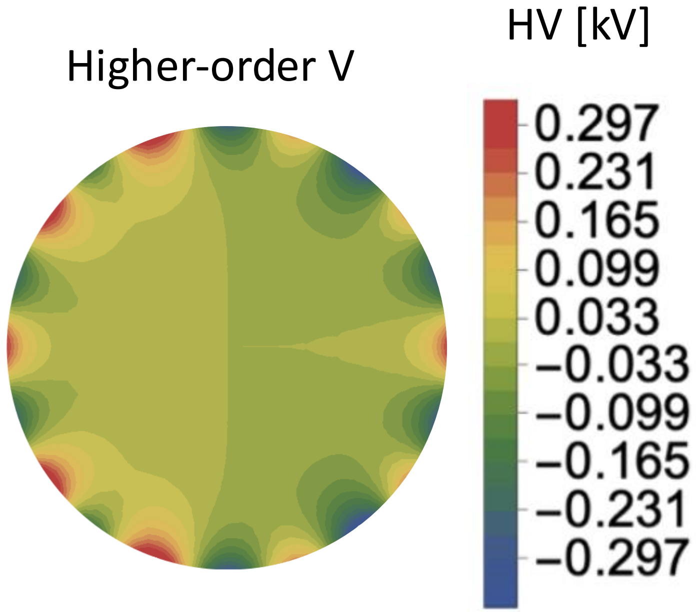

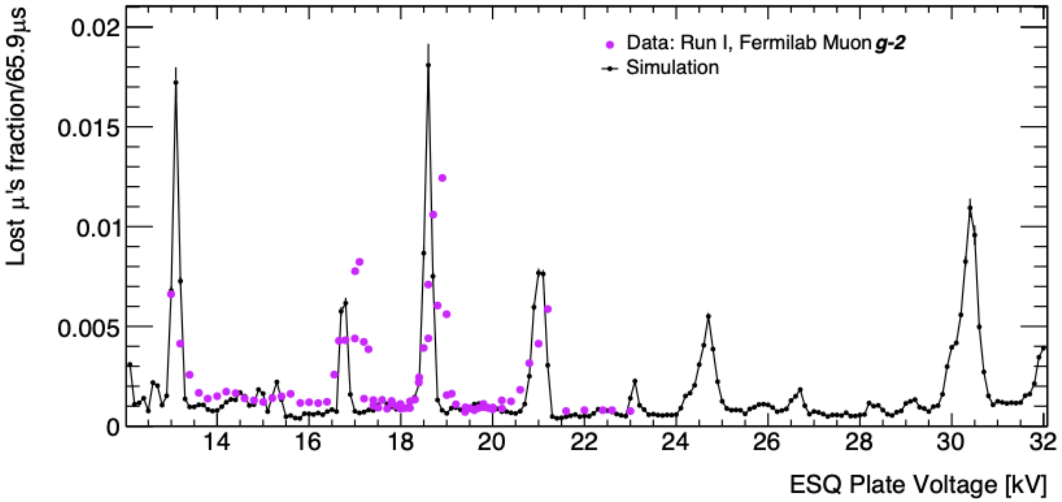

- $3\nu_y = 1$ resonance near operation setpoint. Main driving term from magnetic skew sextupole.

- Beam decoherence ($\tau \approx 190$ μs) driven by electric 20-pole.

Beam Dynamics corrections: Motivation

e: Higher-energy positrons

- Polarized muon beam purpose: To provide ~3GeV positrons out of muon beam decay for calorimetry.

$$\omega_a = \omega_s - \omega_c = -\frac{e}{m} a_\mu \langle B \rangle$$

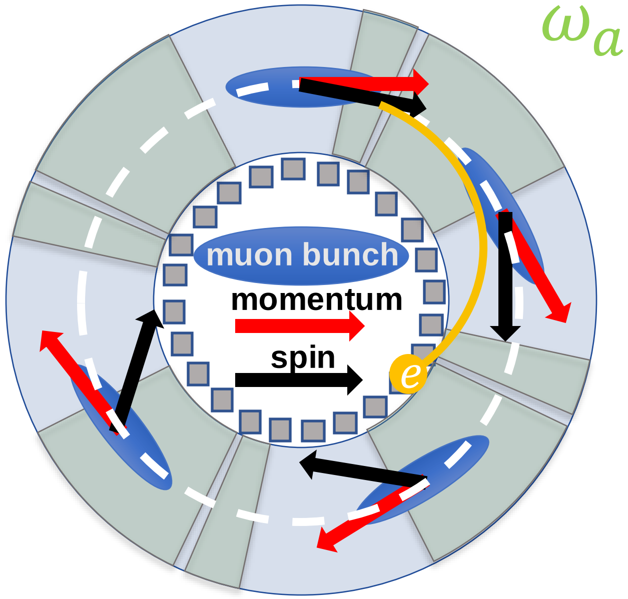

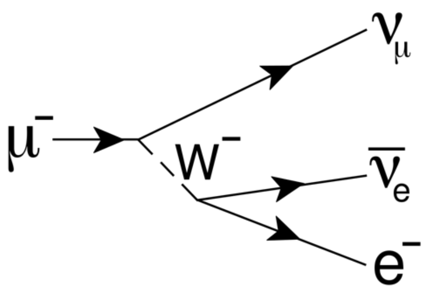

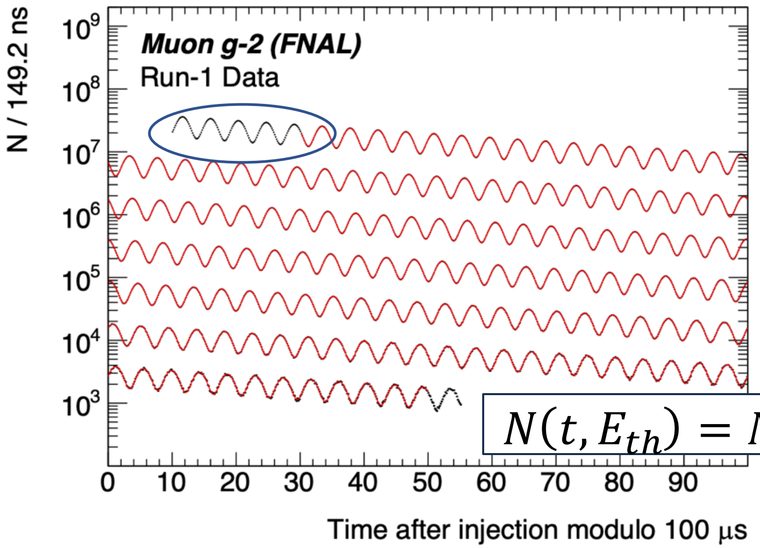

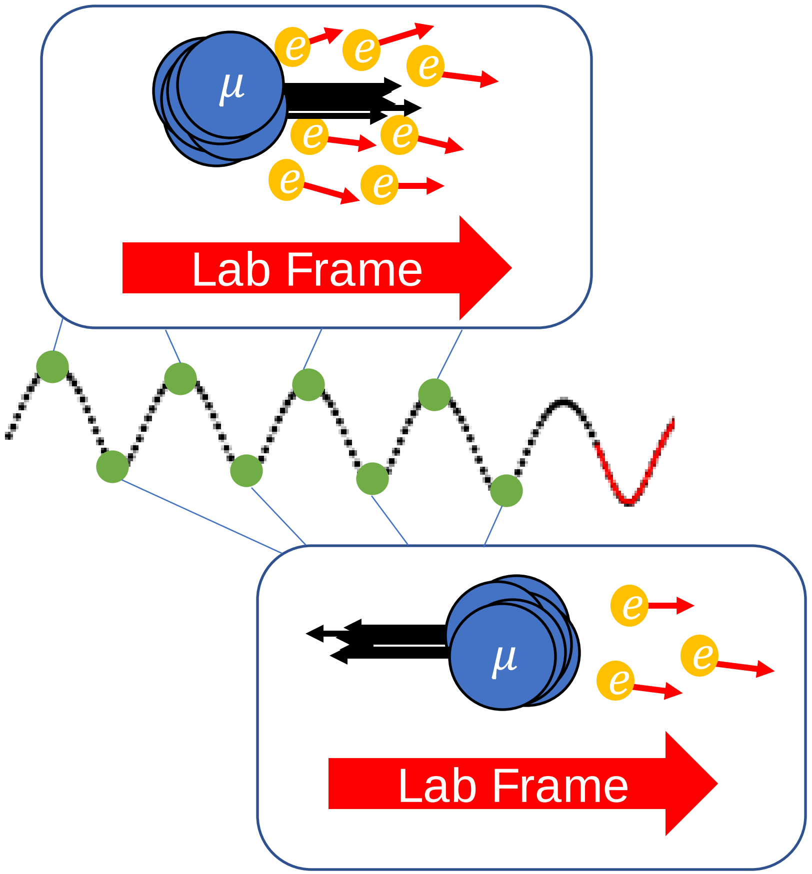

ω_a: Spin precession frequency relative to the momentum direction of muons in the of the storage ring

$$N(t, E_{th}) = N_0(E_{th}) \exp^{-t/\gamma\tau_\mu}[1 + A(E_{th}) \cos(\omega_a t + \varphi_0(E_{th}))]$$

Beam Dynamics corrections: Motivation

e: Higher-energy positrons

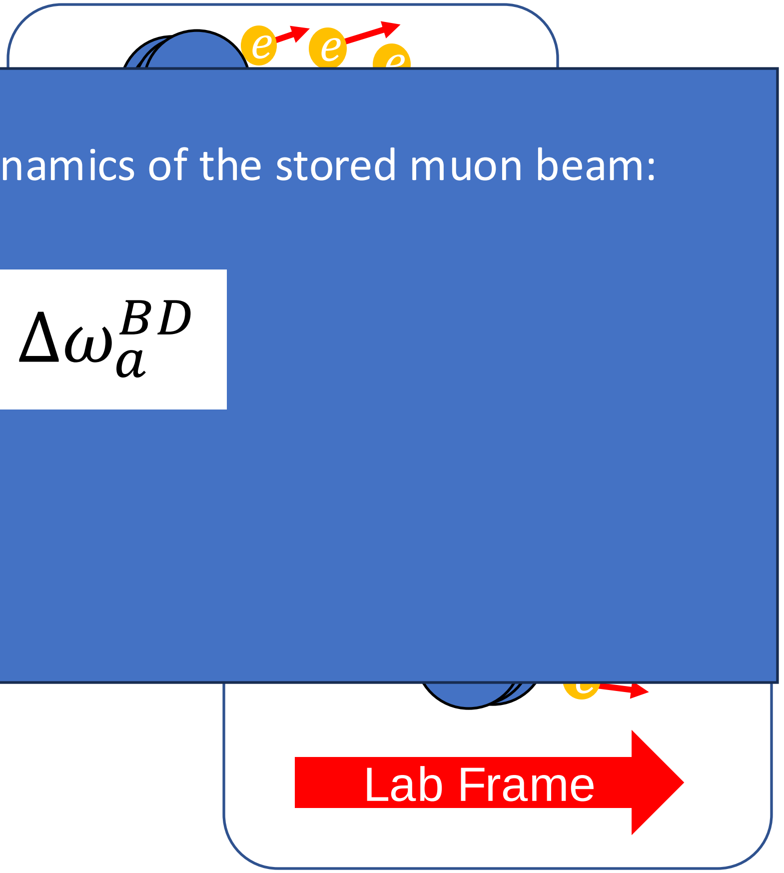

- However, the measured ω_a frequency is biased by the non-ideal dynamics of the stored muon beam:

$$\omega_a = \omega_S - \omega_C = -\frac{e}{m} a_\mu \langle B \rangle + \Delta\omega_a^{BD}$$

- The "Beam Dynamics corrections" account for such biasing.

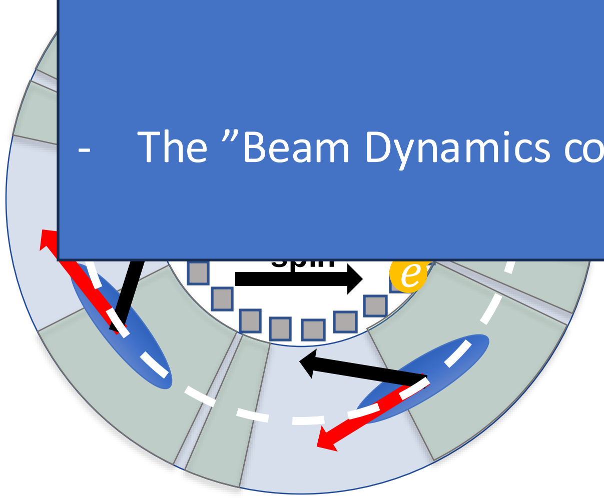

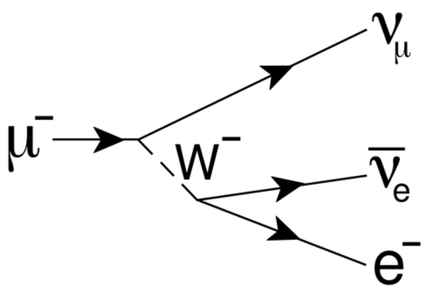

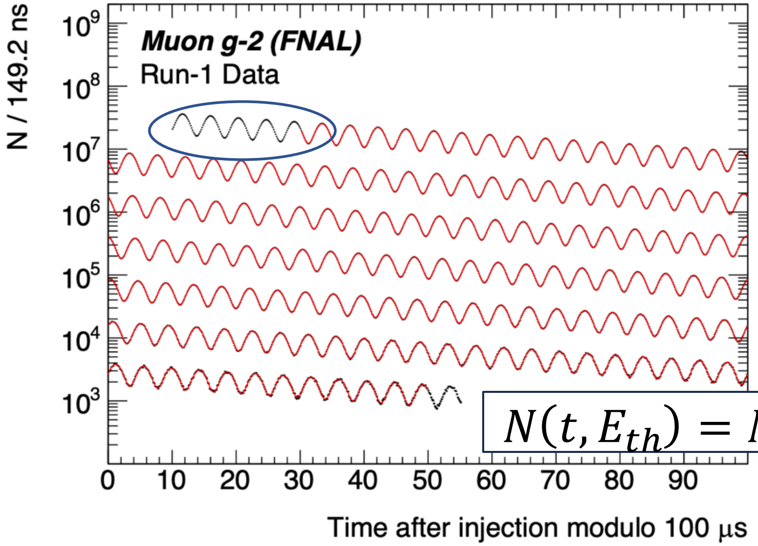

ω_a: Spin precession frequency relative to the momentum direction of muons in the of the storage ring

$$N(t, E_{th}) = N_0(E_{th}) \exp^{-t/\gamma\tau_\mu}[1 + A(E_{th}) \cos(\omega_a t + \varphi_0(E_{th}))]$$

Beam dynamics systematic effects

Nonnegligible when:

- Muon collimation changes overall phase (C_{ml}). [5 ---> 3 ppb]
- Muon beam drifts during measurement (C_{pa}). **[75 ---> 13 ppb]**
- Muon's energy-dependent decay changes overall phase (C_{dd}). [- ---> 17 ppb]

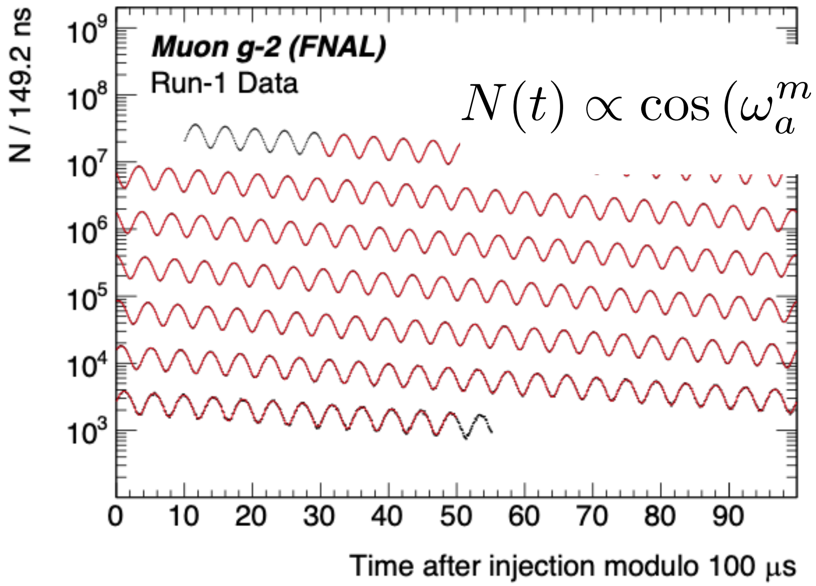

$$N(t) \propto \cos\left(\omega_a^m t + \varphi_0(t)\right) = \cos\left(\omega_a\left[1 + \left\langle\frac{\Delta\omega_a}{\omega_a}\right\rangle + \frac{1}{\omega_a}\frac{d\varphi_0}{dt}\right]t + \varphi_0 + \cdots\right)$$

$$\frac{\mathrm{d}\mathbf{S}}{\mathrm{d}t} = \boldsymbol{\omega}_s \times \mathbf{S}\,, \quad \boldsymbol{\omega}_s = -\frac{q}{m}\left[\left(a + \frac{1}{\gamma}\right)\mathbf{B} - a\frac{\gamma}{\gamma+1}(\boldsymbol{\beta}\cdot\mathbf{B})\boldsymbol{\beta} - \left(a + \frac{1}{\gamma+1}\right)\frac{\boldsymbol{\beta}\times\mathbf{E}}{c}\right]$$

Nonnegligible when:

- Muon beam has nonzero momentum spread (C_e). **[53 ---> 32 ppb]**
- Muons exhibit vertical oscillations (C_p). [13 ---> 10 ppb]

$$\omega_a \approx \omega_a^m\left[1 + C_e + C_p + C_{pa} + C_{dd} + C_{ml}\right]$$

E-field correction

Pitch correction

Phase acceptance correction

Differential decay correction

Muon loss correction

*Run-1 vs. Run-2/3 systematic errors in red.

Beam dynamics systematic effects: *E*-field correction (C_e)

- The *E*-field correction depends on the muon momentum distribution ---> $C_e = \frac{n\beta^2}{1-n} 2\langle\delta^2\rangle \approx 480\ \mathrm{ppb}$
- Two methods to reconstruct the momentum distribution from experimental data:

<u>Debunching method</u>

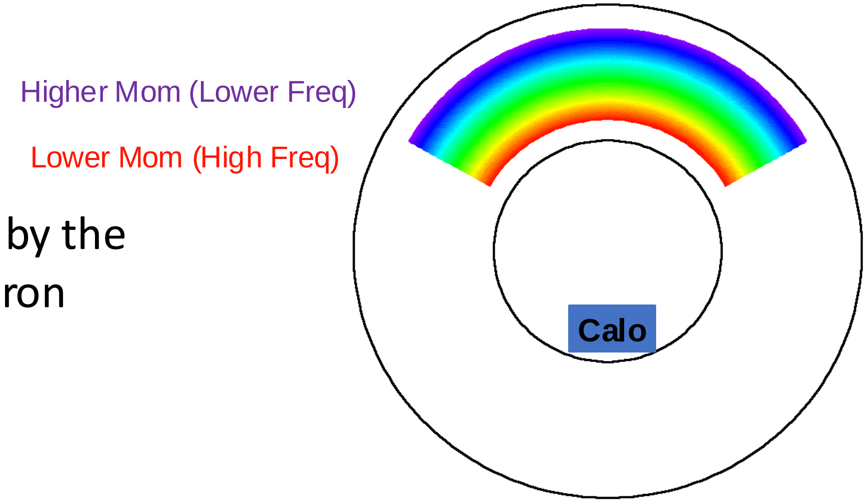

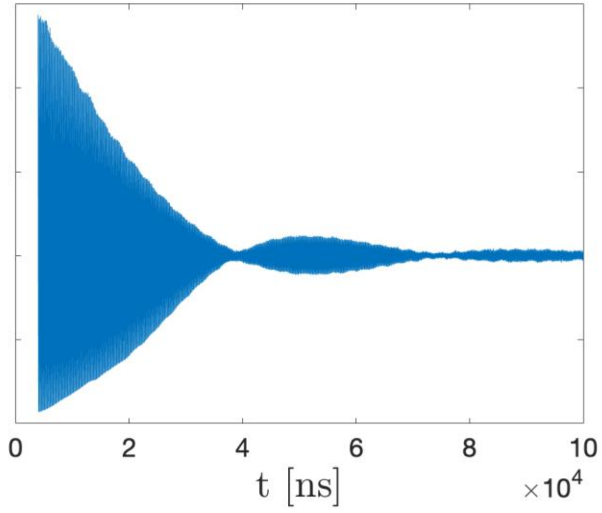

- Fast signal of muons population seen by the calorimeter system builds from cyclotron frequencies distribution.

$$\omega_c \approx \omega_{c0}\left(1 - \frac{1}{1-n}\frac{\Delta p}{p_0}\right)$$

- A time-dependent kick induces the correlation between muon's momentum and time coordinates (under-kick prefers high p, and over-kick prefers low p).

- A **new** χ^2-minimization analysis handles momentum-time correlation.

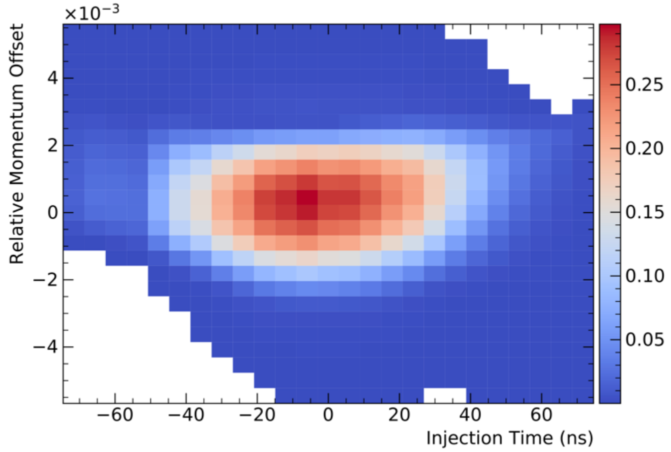

Beam dynamics systematic effects: *E*-field correction (C_e)

- The *E*-field correction depends on the muon momentum distribution ---> $C_e = \frac{n\beta^2}{1-n} 2\langle\delta^2\rangle \approx 480\ \mathrm{ppb}$

- Two methods to reconstruct the momentum distribution from experimental data:

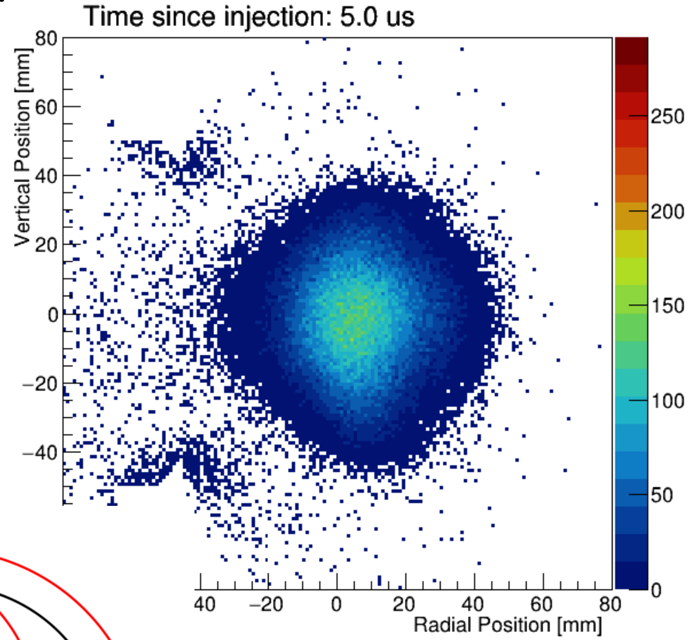

Tracking method

- The tracking system measures the spectrometric behavior of the beam's horizontal motion.

- The narrowing of the beam's width for injection and consequent spread out due to magnetic rigidity is periodically observed (before non-linear decoherence).

$$BR = \frac{p}{e}$$

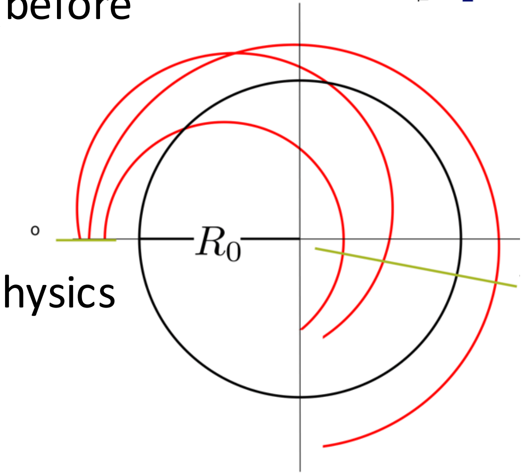

- The momentum spread is reconstructed from a **new** beam-physics analysis (independent of calorimeter data).

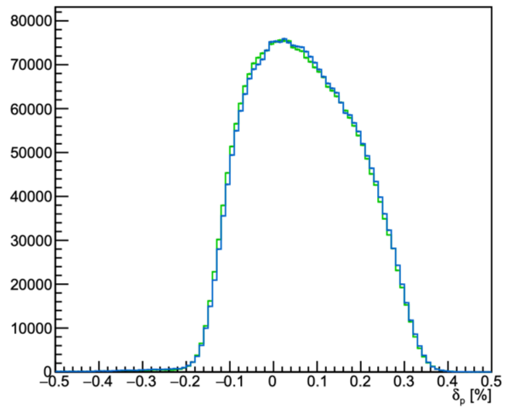

Beam dynamics systematic effects: Pitch correction (C_p)

- The muon's vertical motion (pitch motion) causes the vertical spin precession.

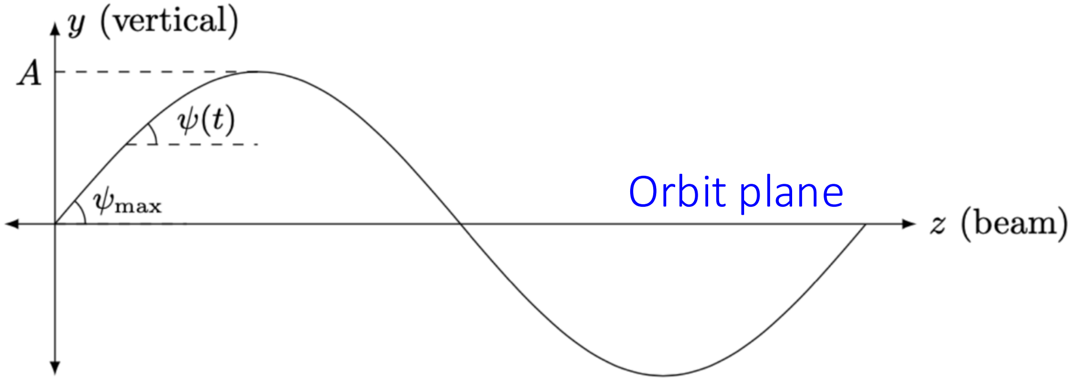

- The horizontal precession (ω_a) is affected by coupled in-plane and out-of-plane precessions due to the vertical motion:

Pitch-driven radial component of $\boldsymbol{\omega}_s$

$$\omega_{sx} \approx \psi_0 \omega_y \sin(\omega_y t + \phi_y),$$

for which case $\omega_a \neq \omega_{cy} - \omega_{sy}$.

$\omega_a \approx 1.44$ rad/μs, $\omega_y \approx 13.8$ rad/μs

$$C_p = \left\langle \frac{\psi_0^2}{4} \left(1 + \frac{\omega_a^2}{\gamma_0^2 (\omega_y^2 - \omega_a^2)} \right) \right\rangle$$

$$\approx \frac{\langle \psi_0^2 \rangle}{4} = \frac{\langle y'^2 \rangle}{2} \approx \frac{n}{2\rho_0^2} \langle y^2 \rangle = \frac{n}{4\rho_0^2} \langle A_y^2 \rangle$$

Beam dynamics systematic effects: Pitch correction (C_p)

- Use the amplitude distribution $\langle A_y^2 \rangle$ instead of the biased vertical distribution $\langle y^2 \rangle$ due to the calorimeter acceptance (the vertical positions are not evenly weighted).
    - The amplitude is reconstructed from the position distribution (acceptance correction included).

Vertical position from tracker data

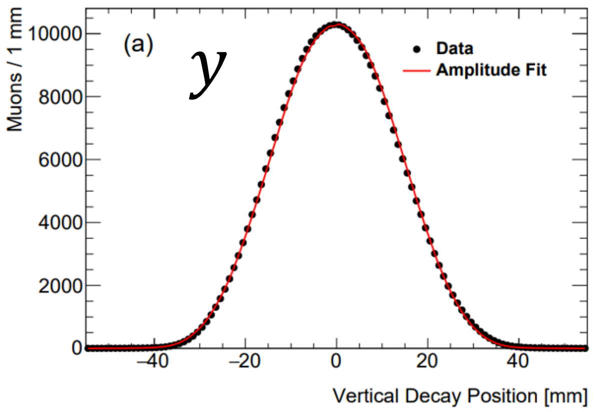

$$C_p = \frac{n}{2\rho_0^2}\langle y^2 \rangle = \frac{n}{4\rho_0^2}\langle A_y^2 \rangle$$

Betatron amplitude

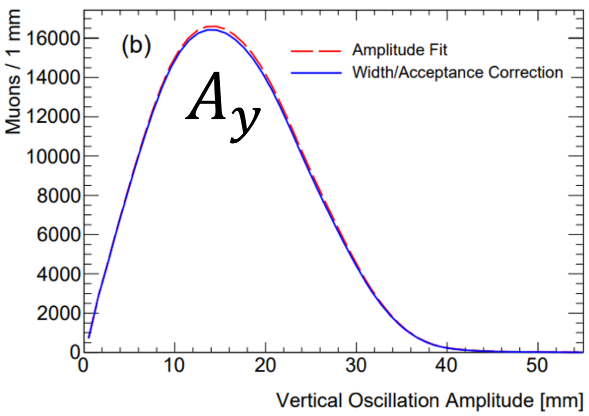

- Tracker alignment and reconstruction dominate the systematic uncertainty.

- Improvement after Run-1: Independent analysis methods to calculate C_p.

Beam dynamics systematic effects: Phase-acceptance correction (C_{pa})

- The g-2 phase of the accepted positrons depends on the muon decay position $\vec{z}$ =(x, y, ϕ) and energy.

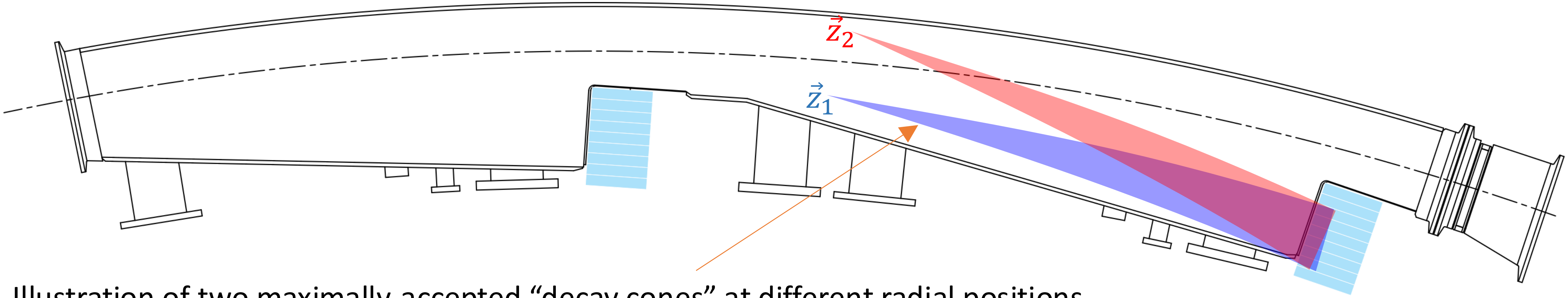

Illustration of two maximally-accepted "decay cones" at different radial positions.

Phase (x, y)

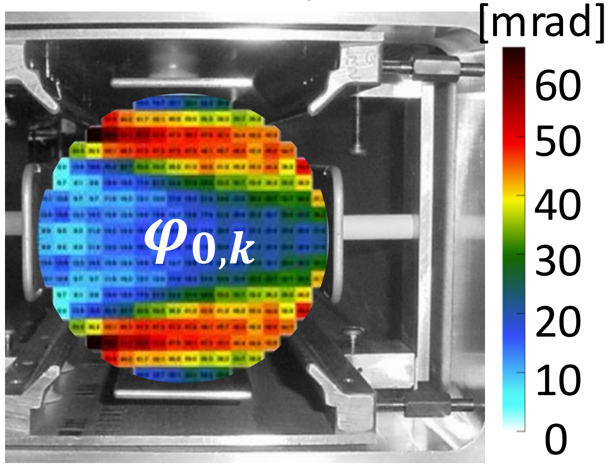

- The g-2 phase carried by a positron is indirectly related by its initial direction due to the parity-violating decay process.

- The phase (prop. to positron direction) that maximizes detection acceptance (prop. to muon decay position) drives the x-y phase dependence.

- This feature itself does not bias ω_a unless the beam profile changes over time.

Beam dynamics systematic effects: Phase-acceptance correction (C_{pa})

- Coherent changes of the transverse muon distribution while the beam depletes drive the phase-acceptance correction:

Phase (x, y)

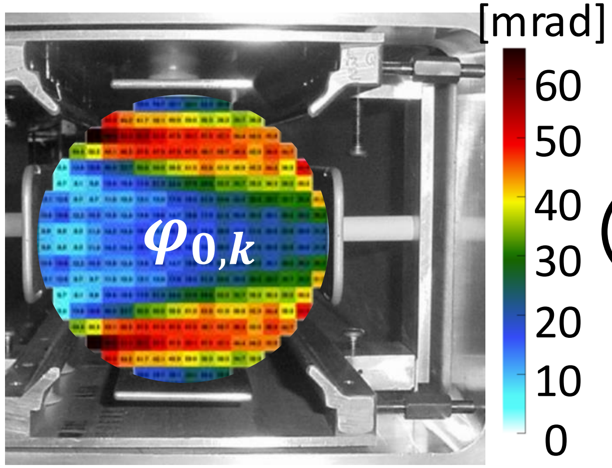

$\otimes$

Muon distribution (x, y, t)

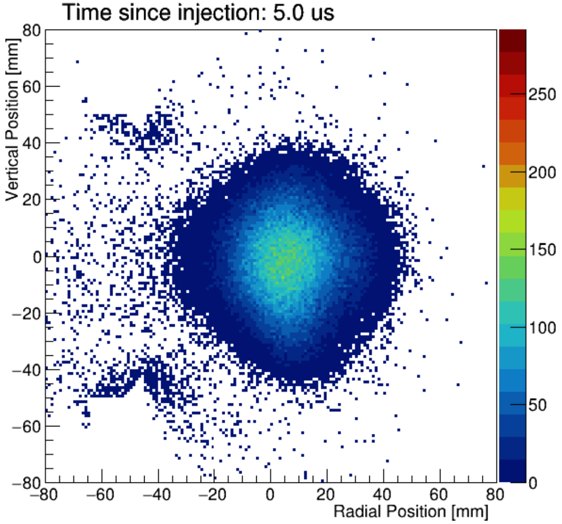

$=$

Phase (t)

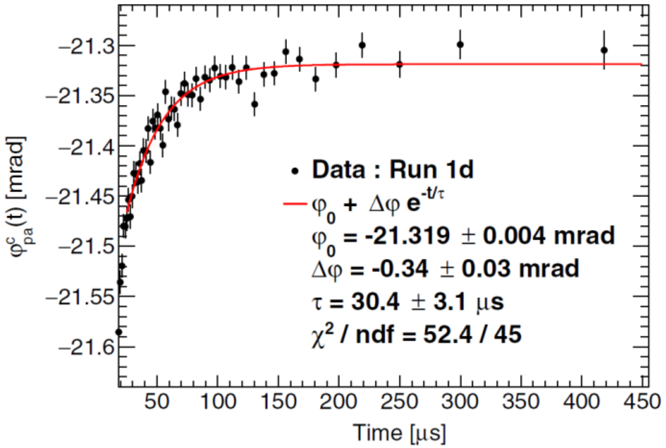

- The dominant effect comes from the vertical width distribution changes.

$$\frac{d\varphi}{dt} \approx \frac{d\varphi}{d\sigma_y} \frac{d\sigma_y}{dt}$$

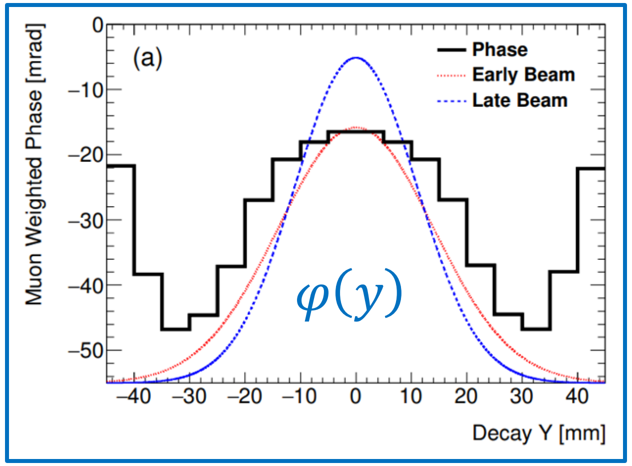

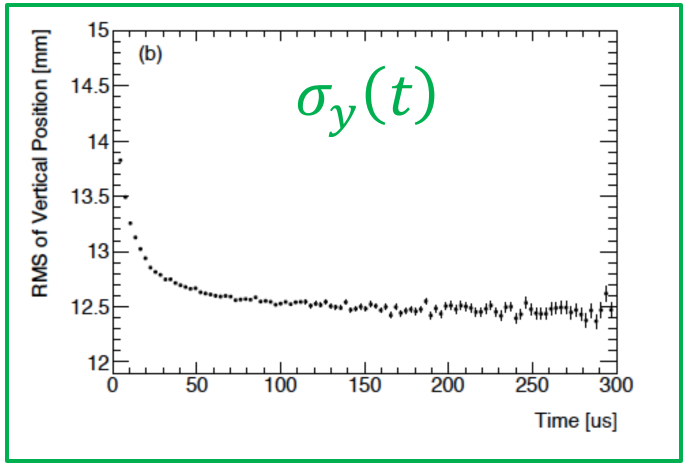

Beam dynamics systematic effects: Phase-acceptance correction (C_{pa})

$$\varphi^c_{pa}(t) = \arctan \frac{\sum_{ij} M^c(x_i, y_j, t) \cdot \varepsilon^c(x_i, y_j) \cdot A^c(x_i, y_j) \cdot \sin(\varphi^c_{pa}(x_i, y_j))}{\sum_{ij} M^c(x_i, y_j, t) \cdot \varepsilon^c(x_i, y_j) \cdot A^c(x_i, y_j) \cdot \cos(\varphi^c_{pa}(x_i, y_j))}$$

Decay distribution (t): $M^c(x_i, y_j, t)$

Asymmetry: $A^c(x_i, y_j)$

Acceptance: $\varepsilon^c(x_i, y_j)$

Calo-detected phase: $\varphi^c_{pa}(x_i, y_j)$

- The calorimeter-dependent detection acceptance and asymmetry information are incorporated to compute the time-varying average phase.
- In Run-1, the phase-acceptance effect was amplified by the damaged ESQ resistors.
  - The damaged resistors were replaced before Run-2.
  - It significantly improved the beam's early-to-late stability, and so did C_{pa} and ΔC_{pa} accordingly.

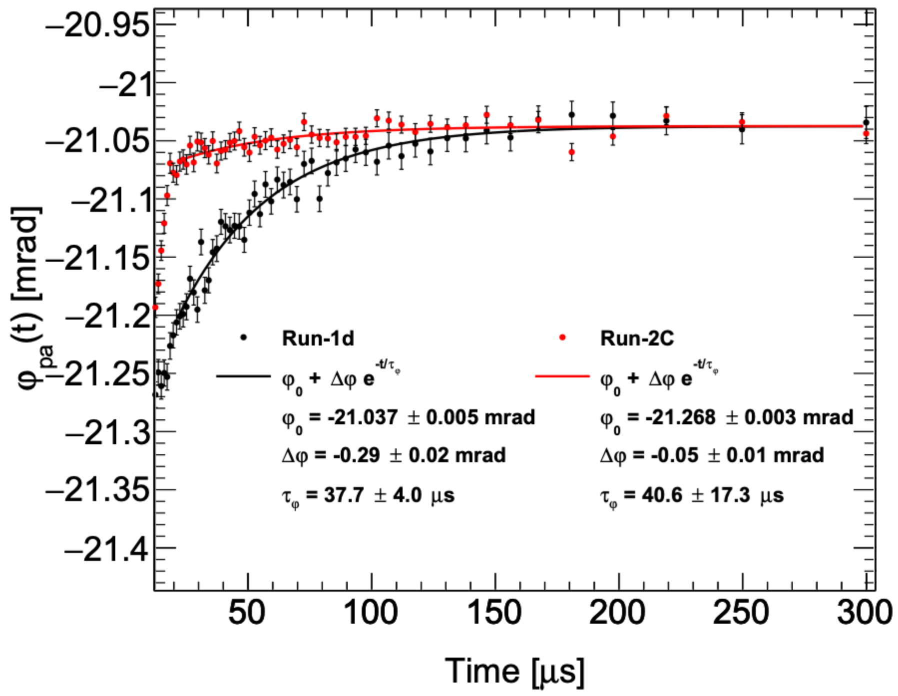

Beam dynamics systematic effects: Differential-decay correction (C_{dd})

- As low-momentum muons decay faster than high-momentum muons, the average momentum of the beam steadily grows over time.

- Correlations between the g-2 Phase and stored muon's momentum coordinates could induce a biasing on ω_a^m.

$$C_{dd} = -\frac{1}{\omega_a}\left(\frac{d\varphi_0}{dt}\right)_{dd} \quad , \quad \left(\frac{d\varphi_0}{dt}\right)_{dd} = \frac{d\varphi_0}{dp}\left(\frac{dp}{dt}\right)_{dd} \approx \frac{d\varphi_0}{d\delta}\frac{1}{\gamma_0\tau_\mu}\sigma_\delta^2$$

$\delta(t > 0) > \delta(t = 0)$

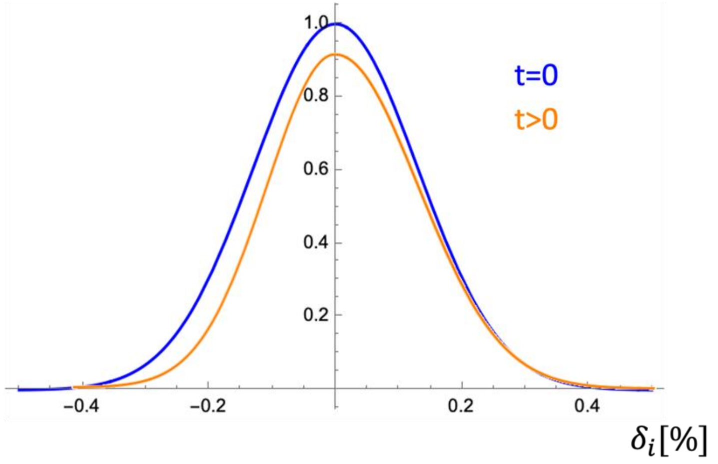

- The momentum-phase correlation can be decomposed into three components:
  - Beamline
    Upstream dipole bending magnet.
  - p-x
    Inflector geometry (especially radial coordinates).
  - p-t_0
    Head-to-tail phase difference &
    Head-to-tail stored momentum distribution.

Beam dynamics systematic effects: Differential-decay correction (C_{dd})

$$\frac{d\phi_0}{dp} = \frac{\partial\phi_0}{\partial x}\frac{dx}{dp} + \frac{\partial\phi_0}{\partial x'}\frac{dx'}{dp} + \frac{\partial\phi_0}{\partial y}\frac{dy}{dp} + \frac{\partial\phi_0}{\partial y'}\frac{dy'}{dp} + \frac{\partial\phi_0}{\partial t_0}\frac{dt_0}{dp} + \frac{\partial\phi_0}{\partial p}$$

$p - x$

$$C_{dd}^{p\text{-}x} = \frac{\sigma_\delta^2}{\omega_a\gamma_0\tau_\mu}\left(\frac{\partial\varphi_0}{\partial x}\frac{dx}{d\delta} + \frac{\partial\varphi_0}{\partial x'}\frac{dx'}{d\delta}\right)$$

$$C_{dd}^{p-x} = -5 \pm 6\,\mathrm{ppb}$$

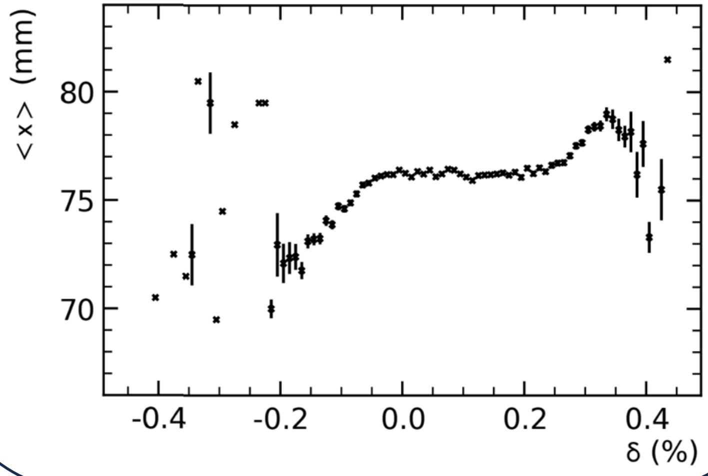

$p - t_0$

$$C_{dd}^{p\text{-}t_0} = \frac{1}{\omega_a}\frac{\partial\varphi_0}{\partial t_0}\frac{dt_0}{dp}\frac{dp}{dt} \approx \frac{\sigma_\delta^2}{\gamma_0\tau_\mu}\frac{dt_0}{d\delta}$$

	$C_{dd}^{p\text{-}t_0}$ [ppb]	$\Delta C_{dd}^{p\text{-}t_0}$ [ppb]
Run-2	6	15
Run-3a	0	16
Run-3b	23	17

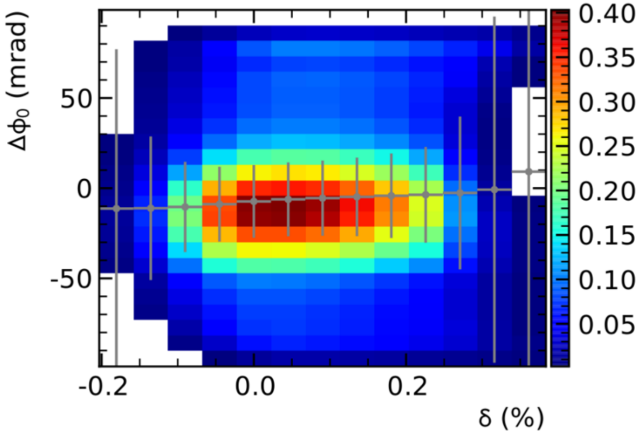

Beamline effect

$$C_{dd}^{bl} = \frac{1}{\omega_a}\frac{\partial\varphi_0}{\partial p}\frac{dp}{dt} \approx \frac{\sigma_\delta^2}{\omega_a\gamma_0\tau_\mu}\frac{\partial\varphi_0}{\partial\delta}$$

	C_{dd}^{bl} [ppb]	ΔC_{dd}^{bl} [ppb]
Run-2	-12	3
Run-3a	-17	3
Run-3b	-20	3

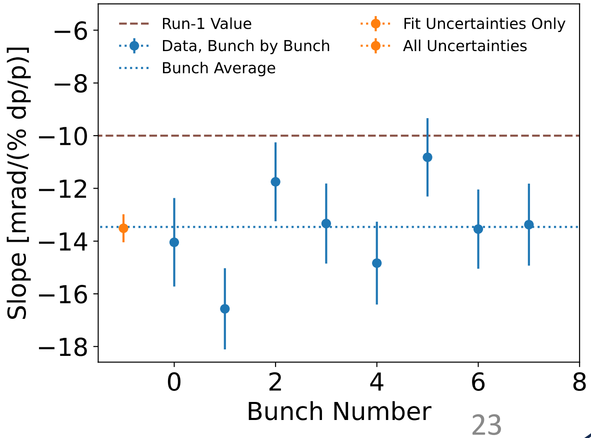

Summary

- A combination of beam preparation, injection, collimation, and storage provided the means to reach the experiment's precision goal.

- The highly uniform magnetic field and electric focusing system allowed for a uniform evolution of the muons' spin precession and cyclotron frequencies.

- Momentum spread and vertical betatron motion introduced additional spin dynamics. Also, detection effects bias the measured anomalous precession frequency.

- With well-established beam dynamics corrections, effects are quantified and applied to the experimental measurements.

BD Corrections [ppb]	Run-1	Run-2/3
C_e	489 ± 53	451 ± 32
C_p	180 ± 13	170 ± 10
C_{pa}	-158 ± 75	-27 ± 13
C_{dd}	-	-15 ± 17
C_{ml}	-11 ± 5	0 ± 3
Sum	$\mathbf{500 \pm 93}$	$\mathbf{580 \pm 40}$

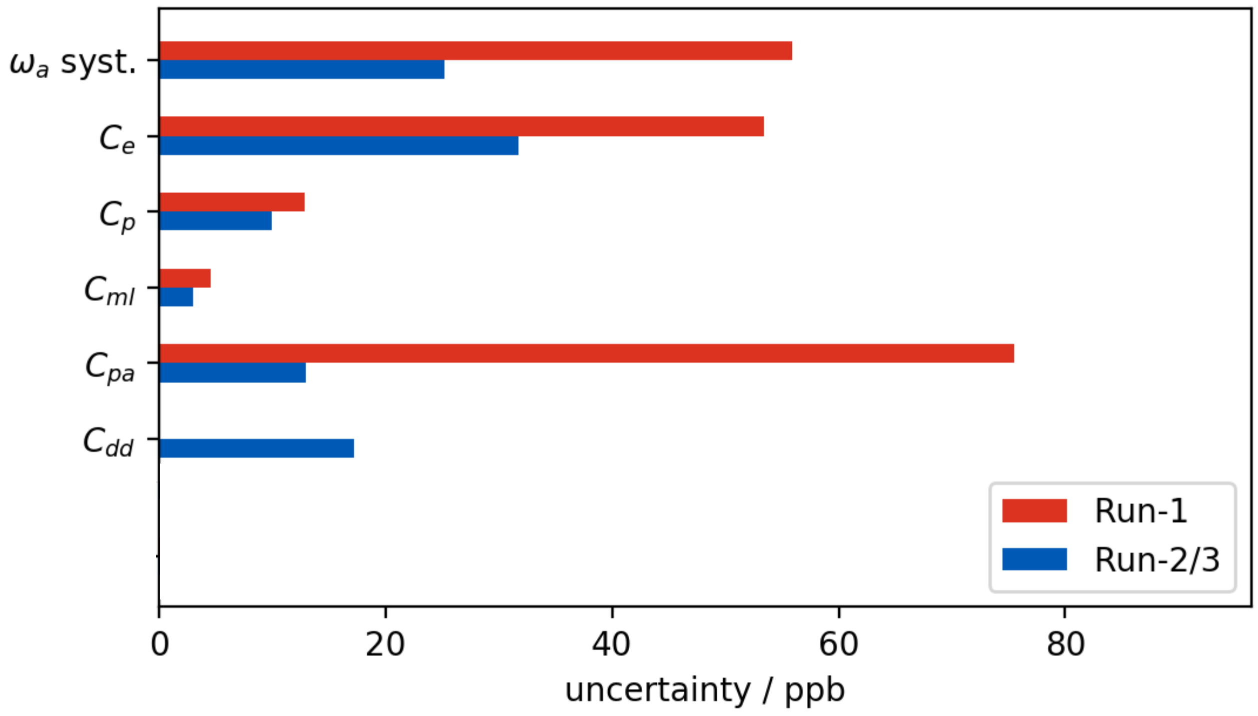

THANKS!